THE JOURNAL OF PHYSICAL CHEMISTRY Letters

Letter

pubs.acs.org/JPCL

Electronic State-Resolved Electron–Phonon Coupling in an Organic Charge Transfer Material from Broadband Quantum Beat Spectroscopy

Aaron S. Rury,* Shayne Sorenson, Eric Driscoll, and Jahan M. Dawlaty*

Department of Chemistry, University of Southern California, Los Angeles, California 90089, United States

Supporting Information

ABSTRACT: The coupling of electron and lattice phonon motion plays a fundamental role in the properties of functional organic charge-transfer materials. In this Letter we extend the use of ultrafast vibrational quantum beat spectroscopy to directly elucidate electron–phonon coupling in an organic charge-transfer material. As a case study, we compare the oscillatory components of the transient reflection (TR) of a broadband probe pulse from single crystals of quinhydrone, a 1:1 cocrystal of hydroquinone and p-benzoquinone, after exciting nonresonant impulsive stimulated Raman scattering and resonant electronic transitions using ultrafast pulses. Spontaneous resonance Raman spectra confirm the assignment of these oscillations as coherent lattice phonon excitations. Fourier transforms of the vibrational quantum beats in our broadband TR measurements allow construction of spectra that we show report the ability of these phonons to directly modulate the electronic structure of quinhydrone. These results demonstrate how coherent ultrafast processes can characterize the complex interplay of charge transfer and lattice motion in materials of fundamental relevance to chemistry, materials sciences, and condensed matter physics.

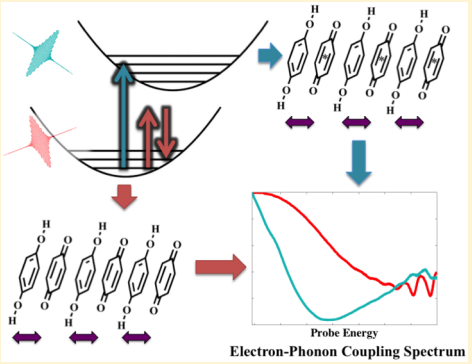

Electron–phonon (e-ph) coupling plays a significant role in functional crystalline organic charge-transfer (CT) materials. The significance of e-ph coupling in organic CT materials physically stems from the ability of intermolecular lattice phonons to directly modulate the distance between electron donor and acceptor molecules. Changes in molecular separation then modulate the charge transfer integral, *t*, which can dramatically impact the electronic structure of a material. The emergence of phonon-driven molecular dimerization between electron donor and acceptor drives these materials into ferroelectric[1] and coupled magnetic-ferroelectric phases[2] as well as charge ordered and charge density wave states.[3,4] Additionally, optical pulses have been shown to cause certain photoinduced phase transitions[5−9] in organic CT materials that have all been shown to rely on significant e-ph coupling.

Despite its importance in material functions and applications, e-ph coupling remains difficult to directly measure, especially using optical spectroscopy. Thus, it has remained a relatively unexplored property of organic CT materials. Bozio and co-workers have shown that resonance Raman (rR) spectroscopy provides an avenue to quantify e-ph coupling in CT materials for which other physical constants such as the on-site electron repulsion and electron-molecular vibration coupling constants are known.[10,11] However, the use of rR spectroscopy to characterize e-ph coupling necessitates measuring the Raman excitation profile in the region of the optically allowed CT transitions to *indirectly* assess e-ph coupling. Thus, this technique to characterize e-ph coupling in these materials has not proliferated.

Ultrafast spectroscopic techniques have shown the ability to investigate the coupling of electronic and nuclear degrees of freedom of a wide range of molecules and molecular materials. As an example, Luer et al. were able to extract the Huang–Rhys factors of the radial breathing and *G* modes of semiconducting carbon nanotubes from vibrational quantum beats observed in degenerate pump–probe measurements using sub-10 fs pulses.[12] However, the use of these vibrational quantum beats to assess e-ph coupling in other types of molecular materials remains unexplored.

In this Letter, we extend the technique of quantum beat spectroscopy to *directly* investigate the electron–phonon coupling of an organic CT crystal in both its ground and excited electronic states. To achieve this, we measure nondegenerate broadband, ultrafast transient reflectivity (TR) spectra of the 1:1 cocrystal of hydroquinone (HQ) and p-benzoquinone (BQ), known as quinhydrone, resonantly probed in its CT absorption band with a white light continuum probe pulse. Quinhydrone is an excellent model material for this experiment since it forms easily from an evaporating solution and possesses an optically induced electron transfer transition that bridges the visible and near-IR regions of the

Received: August 5, 2015
Accepted: August 24, 2015

DOI: 10.1021/acs.jpclett.5b01706
J. Phys. Chem. Lett. 2015, 6, 3560−3564

electromagnetic spectrum. Using excitation higher in energy than the peak of quinhydrone's CT band at 2.64 eV and excitation below its CT band at 0.95 eV, we compare resonant transient reflectivity (rTR) and nonresonant transient reflectivity (nrTR) signals, respectively, to understand differences in the e-ph coupling of quinhydrone as a function of electronic state. Impulsive excitation in both processes results in coherent oscillations in the TR signals. In conjunction with temperature-dependent spontaneous resonance Raman measurements with visible excitation, we propose that three frequencies observed in the measurements represent coherent lattice phonon excitations. These coherent phonon excitations act as an ultrafast modulation of the measured signal in each experiment. Using Fourier analysis and the broadband nature of our measurements, we construct e-ph coupling spectra that use the vibrational modulation provided by the coherent phonons to interrogate the electronic structure of quinhydrone.

Quinhydrone was first discovered in 1844,[13] and its two crystal forms were elucidated by X-ray crystallography several decades ago.[14,15] A schematic of the arrangement of HQ−BQ pairs in monoclinic quinhydrone is shown in the left panel of Figure 1. The HQ−BQ pairs are arranged in tilted linear chains

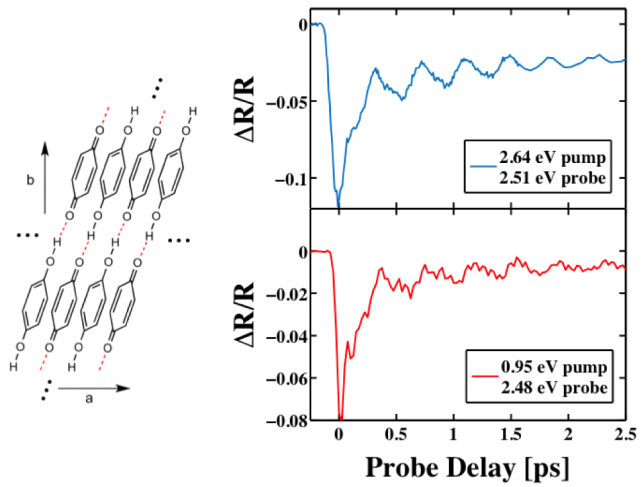

Figure 1. Left: Schematic of the crystalline arrangement of hydroquinone and p-benzoquinone in quinhydrone showing the *a* and *b*-axes as well as interchain hydrogen bonded as red dashes. Top Right: Kinetic slice of the rTR spectra taken at a probe energy of 2.51 eV showing representative oscillations observed across the rTR spectrum. Bottom Right: Kinetic slice of the nrTR spectra taken at a probe energy of 2.48 eV showing representative oscillations observed across the nrTR spectrum.

with a face-to-face separation of 3.22 Å.[15] In addition to the 1D, chain-like arrangement of electron acceptor and donor molecules, the oxygen-bound protons of HQ predominantly hydrogen bond to BQ in an interchain arrangement, shown as red dashed lines in the left panel of Figure 1. As a material that possesses both ground state intermolecular hydrogen bonding and electron transfer interactions, the coupling of electronic and nuclear degrees of freedom in quinhydrone may provide physical chemical insight into the mechanism by which recently designed organic CT materials stabilize room-temperature ferroelectric phases[16,17] as well as design principles for new multifunctional organic materials. Previous studies have examined the intermolecular interactions of quinhydrone via theoretical methods[18,19] as well as electronic and vibrational spectroscopy.[20−24] However, no study has yet investigated e-ph coupling in quinhydrone, nor have modern ultrafast spectroscopic techniques been applied to this material.

As seen in the Supporting Information (SI), the charge transfer absorption band centers near 2.0 eV with a 0.7 eV full width half-maximum line width. Therefore, our resonant pump at 2.64 eV electronically excites the material, while our nonresonant pump at 0.95 eV does not, based on previous studies.[21] The right panel of Figure 1 compares the kinetic trace of the transiently reflected probe component at 2.51 eV for resonant electronic excitation with a 2.64 eV pump pulse (top) to the transiently reflected probe component at 2.48 eV for nonresonant excitation at 0.95 eV (bottom) at 298 K. The full, broadband TR spectra can be found in the SI. Representative oscillatory behavior stands out in both kinetic traces. While wavepacket motion in the excited electronic state has been shown to give rise to oscillations in the presence of resonant excitation, the main contribution to nrTR comes from Impulsive Stimulated Raman Scattering (ISRS), where the pump induces ground state vibrational coherences in the material.[25]

We characterize the oscillations present in the TR spectra through Fourier transform (FT) analysis and vibrational spectroscopy. For FT analysis, we assess the presence of coherent oscillations by undertaking a singular value decomposition (SVD) of both the rTR and ISRS spectra, as described previously[26] and detailed in the Supporting Information. We show the spectra extracted from the FT of the $\mathbf{U}(t)$ matrix weighted by their associated singular values for each excitation process in the top panel of Figure 2 for Fourier frequencies between 50 and 300 cm^{-1}. One sees that two frequencies dominate the Fourier spectra derived from the rTR spectrum, while at least three frequencies appear in the ISRS spectrum in this spectral region. One observes components at 91 and 172 cm^{-1} in both Fourier spectra and an additional component at 117 cm^{-1} in the spectrum excited by ISRS. A prominent peak also appears in the Fourier spectrum derived from the ISRS process at 450 cm^{-1}, shown in the Supporting Information, near the position of a previously assigned intramolecular BQ ring bending vibration we denote BQ ν_6.[22,27]

To better understand the nature of the two features in both Fourier spectra, we undertook temperature-dependent, polarized resonance Raman (rR) measurements of monoclinic quinhydrone single crystals. The bottom panel of Figure 2 shows rR spectra of quinhydrone for incident and scattered polarizations parallel to the *a*-axis of the crystal for frequencies between 50 and 300 cm^{-1} for five different temperatures ranging from 78 to 273 K excited at 2.33 eV. Five distinct peaks appear in the spectrum cooled to 78 K that we denote ν_1 through ν_5 in order of increasing frequency. At 273 K we observe a broad, complex peak centered at 90 cm^{-1} corresponding to the ν_2 mode, and two more symmetric peaks at 113 and 169 cm^{-1} corresponding to the ν_3 and ν_4 modes, respectively. Based on this naming convention, the top panel of Figure 2 indicates that our resonant pump−probe experiment excites the ν_2 and ν_4 modes while the nonresonant experiment excites the ν_2, ν_3, and ν_4 modes. Given the frequency of these modes and their shift as a function of temperature, we associate their presence in quinhydrone with the electron transfer interaction between the donor and acceptor molecules. As we cool the crystal, all three of these peaks shift upward in frequency, as one would expect when a

DOI: 10.1021/acs.jpclett.5b01706
J. Phys. Chem. Lett. 2015, 6, 3560−3564

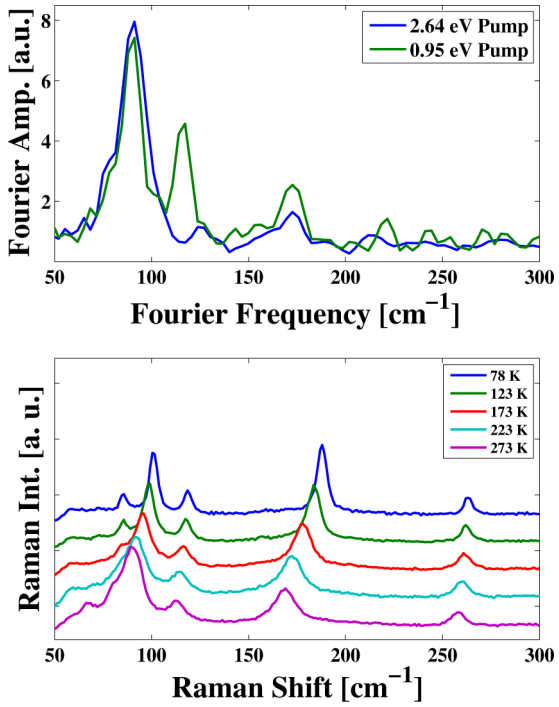

Figure 2. Top: Comparison of the Fourier spectra observed for resonant impulsive excitation at 2.64 eV (blue) to nonresonant impulsive stimulated Raman scattering (ISRS) excitation at 0.95 eV (green). We observe peaks at 91 $^{-1}$ and 172 cm^{-1} in both spectra while the peak at 117 cm^{-1} is only observed in the spectrum excited by ISRS. Bottom: Temperature dependent, polarized resonance Raman scattering spectra in the frequency region between 50 $^{-1}$ and 300 cm^{-1} of monoclinic quinhydrone excited at 2.33 eV. The peaks centered at 90 $^{-1}$, 113 $^{-1}$, and 169 cm^{-1} at 273 K shift to higher frequency and change in intensity upon cooling, motivating their assignment as intermolecular lattice modes.

thermally contracting crystal increases the ground state electron transfer between HQ and BQ.

Comparison of the Fourier spectra to the rR spectra provides an important insight into the optical processes participating in the ultrafast measurements. The ν_3 mode appears in the Fourier spectrum derived from the ISRS measurement as well as the rR spectrum. However, as stated above, this peak does not appear in the Fourier spectrum excited by ultrafast resonant electronic excitation. Since the rR spectra likely derive enhancement from the same optical transition used for the rTR measurements, the absence of the ν_3 mode in the Fourier spectrum for 2.64 eV excitation implies that resonantly enhanced stimulated Raman processes that produce ground state vibrational coherences contribute insignificantly to the observed dynamics in our resonant pump−probe measurements. Therefore, the oscillations imparted on the probe for resonant excitation likely correspond to lattice phonons in the electronic excited state. Also, the presence of the ν_2 and ν_4 in ultrafast resonant excitation points to their appearing in the rR spectra of Figure 2 via a Franck−Condon mechanism, whereas the ν_3 could appear in the rR spectra via a Herzberg−Teller mechanism. The Herzberg−Teller mechanism does not necessitate a displacement of the excited electronic state along a given mode in order to observe the mode in resonance Raman spectroscopy, reducing the likelihood that such a mode would produce a wave packet in an ultrafast resonant transition.

To understand the effect of the coherent vibrational excitations on the electronic structure of quinhydrone, we can cast our results in the context of previous work examining the energy dependence of the amplitude of coherent nuclear motion.[12,28−32] All these studies found that the probe energy dependence of the Fourier amplitude appears as a derivative of the steady-state absorption spectrum when a coherent vibration directly modulates an optical band gap. When one plots the absolute value of the amplitude of the FT, this derivative appears as a dip in the amplitude at the peak energy of the transition. In addition to this line shape in the amplitude, the phase of the coherent oscillation shifts at the energy of the transition.

Guided by these principles, we analyzed our spectra to identify how the pump-induced phonons modulate the charge transfer parameter t of quinhydrone. We took the outer product, (i.e., matrix multiplying), of the singular value-weighted Fourier spectra shown in the top panel of Figure 2 with their associated decomposed spectra found in the matrix $\mathbf{V}^{\dagger}(E)$. The calculated spectrum contains the amplitude of every Fourier component in the coherent oscillations of each ultrafast measurement as a function of the resonant probe energy, thus creating an electron−phonon (e-ph) coupling spectrum. We fully detail the calculation of the e-ph coupling spectrum in the Supporting Information as well as present the full band e-ph coupling spectra for each of the coherent phonons found in the top panel of Figure 2.

Figure 3 compares the e-ph coupling spectra of the ν_2, ν_3, and ν_4 phonons of quinhydrone pumped at 0.95 eV. These spectra show three regions where a dip in the amplitude of the oscillation is coincident with a noticeable shift in its phase: 1.67, 1.62, and 1.54 eV. Additionally, a dip and phase shift appear near 1.52 eV in the e-ph coupling spectra of both the ν_2 and ν_4 modes and near 1.61 eV for only the ν_2 mode. These features indicate that each of the phonons coherently excited by the near-IR ISRS pump modulates t, leading to modulation of an optical transition very likely connected to electron transfer. Given their red-shift relative to the peak of the CT absorption band near 2.0 eV, these features likely correspond to CT excitons of quinhydrone that have remained difficult to characterize, especially at room temperature.

Figure 4 shows the e-ph coupling spectrum of the ν_4 mode upon 2.64 eV excitation as well as its phase. This spectrum shows a minimum just above 2.2 eV in addition to a conspicuous phase shift. This line shape implies that there is an optically allowed transition from the electronic state excited by the 2.64 eV pump pulse to a higher lying state that becomes directly modulated by this phonon mode. The absorption of the probe pulse after 2.64 eV excitation could transfer an electron from BQ to HQ. In such a case, the excited state e-ph coupling spectrum associated with the ν_4 mode and its phase are consistent with the picture that this phonon directly modulates t in an electronic excited state of quinhydrone.

In conclusion, we have used ultrafast rTR and ISRS measurements that probe transitions of the organic CT crystal quinhydrone to determine how different coherent phonon excitations couple to this material's electronic structure. Building off of previous applications of quantum beat and coherent phonon spectroscopy, we used Fourier and singular value decomposition analyses to construct electron−phonon coupling spectra that directly report on the interplay of electronic and nuclear degrees of freedom of this material. With the help of resonance Raman spectroscopy, we show that all

DOI: 10.1021/acs.jpclett.5b01706
J. Phys. Chem. Lett. 2015, 6, 3560−3564

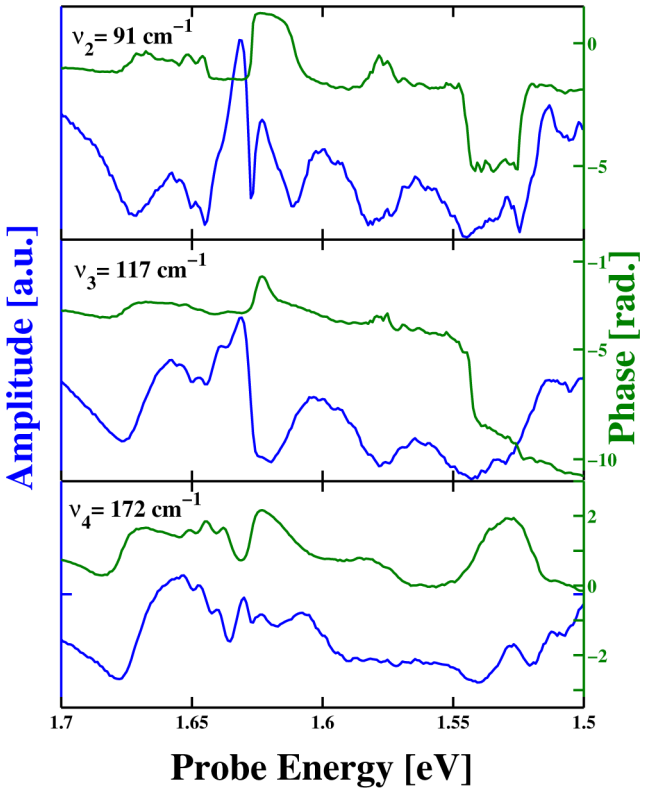

Figure 3. Comparison of the amplitude (blue) to the phase (green) of the e-ph coupling spectra the ν_2, ν_3, and ν_4 modes in the ground electronic state of quinhydrone for probe energies between 1.5 and 1.7 eV. The amplitude and phase of the spectra are consistent with several electronic transitions that could be due to charge transfer excitons in quinhydrone.

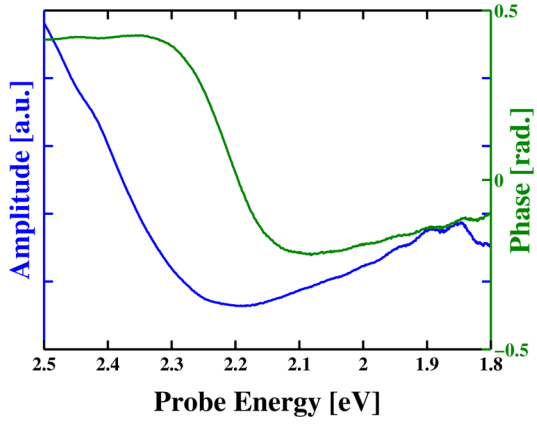

Figure 4. Comparison of the amplitude (blue) to the phase (green) of the e-ph coupling spectrum of the ν_4 mode in the excited electronic state of quinhydrone. The amplitude dip and phase shift around the probe energy of 2.2 eV are consistent with excited state absorption process that becomes modulated by this phonon mode at this energy.

three lattice phonons excited in quinhydrone's ground state modulate near-IR transitions associated with electron transfer that may be excitonic in nature. Using the technique outlined in this study, one could use temperature changes in the quinhydrone crystal to further characterize these transitions and better understand the contributions of excitons to the ground state electronic properties of this material. Also, resonant electronic pumping shows that a lattice vibration near 172 cm^{-1} couples to electron transfer in the excited state of this material. We believe that this technique could be applied to a wide range of organic materials whose properties may include thermoelectricity, superconductivity, as well as other exotic phases in which the coupling of electron transfer and nuclear motion plays a significant role. Further characterization of e-ph coupling in these materials will help in the design of next-generation chemical, electronic, and photonics materials and provide new insights into fundamental physical chemical processes behind their function.

EXPERIMENTAL METHODS

Single crystals of quinhydrone were recrystallized several times from a highly concentrated solution in acetonitrile to produce larger crystals with dimensions on the order of 0.1 × 0.2 × 3 mm elongated along the *a*-axis of the crystal, as shown previously.[14] Broadband, ultrafast resonant transient reflectivity (rTR) and impulsive stimulated Raman scattering (ISRS) spectra were measured using the output of a 1 kHz regenerative amplified Ti:sapphire laser system. An optical parametric amplifier (OPA) system generated the pump pulse for both excitation energies while we focused a separate attenuated beam in a 3 mm thick piece of sapphire to produce the white light continuum (WLC) probe pulse used in both experiments. Transient signals were calculated from single shot pairs of pumped and unpumped reflection spectra measured on a high speed CCD camera (Princeton Instruments Pixis) mounted on a 0.3 m monochromator (iHR 320 Horiba Scientific Instruments). The rTR measurements were made with 100 nJ of pump energy and the ISRS measured with 2 μJ, both focused to a spot on the order of 200 μm while nearly 1 nJ of probe energy focused to a spot of ∼150 μm. To produce a high signal-to-noise 2D contour rTR spectrum as a function of probe time delay, four consecutive time scans were averaged together, while nine such spectra were averaged together to produce the 2D contour ISRS spectrum. The spatial mode of the probe beam reflected from the sample as well as the probe spectrum measured by the CCD camera were checked between each scan to verify the photostability of the sample at these pump and probe powers. In both measurements, the pump and probe pulses were polarized along the crystal's *a*-axis.[21] Temperature-dependent, polarized resonance Raman (rR) spectra were obtained using a Raman microscope (XploRA ONE Horiba Scientific Instruments) fitted with silver block temperature controller (Linkam Scientific Instruments) providing 0.1 K precision between 78 and 850 K.

ASSOCIATED CONTENT

Supporting Information

The steady-state reflectance spectrum of quinhydrone, the 2.64 eV pump pulse and white light continuum pulse, the full 2D resonant and nonresonant transient reflectivity spectra, details related to the singular value decomposition analysis and calculation of the Fourier and electron−phonon coupling spectra as well as figures showing the amplitude and phase of all of the electron−phonon coupling spectra of Figures 3 and 4. The Supporting Information is available free of charge on the ACS Publications website at DOI: 10.1021/acs.jpclett.5b01706.

(PDF)

DOI: 10.1021/acs.jpclett.5b01706
J. Phys. Chem. Lett. 2015, 6, 3560−3564

AUTHOR INFORMATION

Corresponding Authors

*E-mail: arury@usc.edu.

*E-mail: dawlaty@usc.edu

Notes

The authors declare no competing financial interest.

ACKNOWLEDGMENTS

The authors acknowledge support from the University of Southern California start up grant and the AFOSR YIP Award (FA9550-13-1-0128). S.S. was supported by the University of Southern California Provost Fellowship.

REFERENCES

(1) Horiuchi, S.; Tokura, Y. Organic Ferroelectrics. *Nat. Mater.* **2008**, *7*, 357−366.

(2) Kagawa, F.; Horiuchi, S.; Tokunaga, M.; Fujioka, J.; Tokura, Y. Ferroelectricity in a One-Dimensional Organic Quantum Magnet. *Nat. Phys.* **2010**, *6*, 169−172.

(3) Seo, H.; Hotta, C.; Fukuyama, H. Toward Systematic Understanding of Diversity of Electronic Properties in Low-Dimensional Molecular Solids. *Chem. Rev.* **2004**, *104*, 5005−36.

(4) Onda, K.; Yamochi, H.; Koshihara, S.-y. Diverse Photoinduced Dynamics in an Organic Charge-Transfer Complex Having Strong Electron-Phonon Interactions. *Acc. Chem. Res.* **2014**, *47*, 3494−503.

(5) Okamoto, H.; Ishige, Y.; Tanaka, S.; Kishida, H.; Iwai, S.; Tokura, Y. Photoinduced Phase Transition in Tetrathiafulvalene-p-chloranil Observed in Femtosecond Reflection Spectroscopy. *Phys. Rev. B: Condens. Matter Mater. Phys.* **2004**, *70*, 1−18.

(6) Iwai, S.; Okamoto, H. Ultrafast Phase Control in One-Dimensional Correlated Electron Systems. *J. Phys. Soc. Jpn.* **2006**, *75*, 011007.

(7) Onda, K.; Ogihara, S.; Yonemitsu, K.; Maeshima, N.; Ishikawa, T.; Okimoto, Y.; Shao, X.; Nakano, Y.; Yamochi, H.; Saito, G.; et al. Photoinduced Change in the Charge Order Pattern in the Quarter-Filled Organic Conductor $(EDO\text{-}TTF)_2PF_6$ with a Strong Electron-Phonon Interaction. *Phys. Rev. Lett.* **2008**, *101*, 2−5.

(8) Miyamoto, T.; Kimura, K.; Hamamoto, T.; Uemura, H.; Yada, H.; Matsuzaki, H.; Horiuchi, S.; Okamoto, H. Measurement of a Photoinduced Transition from a Nonordered Phase to a Transient Ordered Phase in the Organic Quantum-Paraelectric Compound Dimethyltetrathiafulvalene-dibromodichloro-p-benzoquinone using Femtosecond Laser Irradiation. *Phys. Rev. Lett.* **2013**, *111*, 187801.

(9) Takubo, N.; Tajima, N.; Yamamoto, H. M.; Cui, H.; Kato, R. Lattice Distortion Stabilizes the Photoinduced Metallic Phase in the Charge-Ordered Organic Salts $(BEDT\text{-}TTF)_3X_2$ (X = ReO_4, ClO_4). *Phys. Rev. Lett.* **2013**, *110*, 227401.

(10) Bozio, R.; Feis, A.; Zanon, I.; Pecile, C. Resonance Raman Scattering of a Peierls-Hubbard Dimer. *J. Chem. Phys.* **1989**, *91*, 13.

(11) Pedron, D.; Speghini, A.; Mulloni, V.; Bozio, R. Coupling of Electrons to Intermolecular Phonons in Molecular Charge Transfer Dimers: A Resonance Raman Study. *J. Chem. Phys.* **1995**, *103*, 2795.

(12) Lüer, L.; Gadermaier, C.; Crochet, J.; Hertel, T.; Brida, D.; Lanzani, G. Coherent Phonon Dynamics in Semiconducting Carbon Nanotubes: A Quantitative Study of Electron-Phonon Coupling. *Phys. Rev. Lett.* **2009**, *102*, 127401.

(13) Stahly, G. P. A Survey of Cocrystals Reported Prior to 2000. *Cryst. Growth Des.* **2009**, *9*, 4212−4229.

(14) Sakurai, T. The Crystal Structure of the Triclinic Modification of Quinhydrone. *Acta Crystallogr.* **1965**, *19*, 320−330.

(15) Sakurai, T. On the Refinement of the Crystal Structures of Phenoquinone and Monoclinic Quinhydrone. *Acta Crystallogr., Sect. B: Struct. Crystallogr. Cryst. Chem.* **1968**, *24*, 403−412.

(16) Tayi, A. S.; Shveyd, A. K.; Sue, A. C.-H.; Szarko, J. M.; Rolczynski, B. S.; Cao, D.; Kennedy, T. J.; Sarjeant, A. a.; Stern, C. L.; Paxton, W. F.; et al. Room-temperature Ferroelectricity in Supramolecular Networks of Charge-Transfer Complexes. *Nature* **2012**, *488*, 485−489.

(17) D'Avino, G.; Verstraete, M. J. Are Hydrogen-Bonded Charge Transfer Crystals Room Temperature Ferroelectrics? *Phys. Rev. Lett.* **2014**, *113*, 237602.

(18) Barone, V.; Cacelli, I.; Crescenzi, O.; d'Ischia, M.; Ferretti, A.; Prampolini, G.; Villani, G. Unraveling the Interplay of Different Contributions to the Stability of the Quinhydrone Dimer. *RSC Adv.* **2014**, *4*, 876.

(19) González Moa, M. J.; Mandado, M.; Mosquera, R. A. A Computational Study on the Stacking Interaction in Quinhydrone. *J. Phys. Chem. A* **2007**, *111*, 1998−2001.

(20) Fukushima, K.; Sakurada, M. Lattice Vibrations of Quinhydrone and the Intermolecular Potential in the Crystal. *J. Phys. Chem.* **1976**, *80*, 1367−1373.

(21) Mitani, T.; Saito, G.; Urayama, H. Cooperative Phenomena Associated with Electron and Proton Transfer in Quinhydrone Charge-Transfer Crystal. *Phys. Rev. Lett.* **1988**, *60*, 2299−2302.

(22) Kubinyi, M.; Keresztury, G. Infrared and Raman Spectroscopic Study of Molecular Interactions in Quinhydrone Crystals. *Spec. Acta* **1989**, *45*, 421−429.

(23) Kalninsh, K.; Gadonas, R.; Krasauskas, V.; Pugzhlys, A. Thermal and Photo-Stimulated Hydrogen Atom Transfer in Quinhydrones. *Chem. Phys. Lett.* **1993**, *209*, 63−66.

(24) Kanesaka, I.; Nagami, H.; Kobayashi, K.; Ohno, K. Infrared Intensity Study on Molecular Interactions in Quinhydrone. *Bull. Chem. Soc. Jpn.* **2006**, *79*, 406−412.

(25) Ruhman, S.; Joly, A. G.; Nelson, K. A. Time-Resolved Observations of Coherent Molecular Vibrational Motion and the General Occurrence of Impulsive Stimulated Scattering. *J. Chem. Phys.* **1987**, *86*, 6563−6565.

(26) Ernsting, N. P.; Kovalenko, S. A.; Senyushkina, T.; Saam, J.; Farztdinov, V. Wave-Packet-Assisted Decomposition of Femtosecond Transient Ultraviolet-Visible Absorption Spectra:? Application to Excited-State Intramolecular Proton Transfer in Solution. *J. Phys. Chem. A* **2001**, *105*, 3443−3453.

(27) Dunn, T.; Francis, A. The Ground State Fundamentals of p-Benzoquinone and p-Benzoquinone-d_4. *J. Mol. Spectrosc.* **1974**, *50*, 1−13.

(28) Kumar, A. T. N.; Rosca, F.; Widom, A.; Champion, P. M. Investigations of Amplitude and Phase Excitation Profiles in Femtosecond Coherence Spectroscopy. *J. Chem. Phys.* **2001**, *114*, 701−724.

(29) Kano, H.; Saito, T.; Kobayashi, T. Observation of Herzberg-Teller-Type Wave Packet Motion in Porphyrin J-Aggregates Studied by Sub-5-fs Spectroscopy. *J. Phys. Chem. A* **2002**, *106*, 3445−3453.

(30) Ishii, N.; Tokunaga, E.; Adachi, S.; Kimura, T.; Matsuda, H.; Kobayashi, T. Optical Frequency- and Vibrational Time-Resolved Two-Dimensional Spectroscopy by Real-Time Impulsive Resonant Coherent Raman Scattering in Polydiacetylene. *Phys. Rev. A: At., Mol., Opt. Phys.* **2004**, *70*, 023811.

(31) Kobayashi, T.; Wang, Z. Spectral Oscillation in Optical Frequency-Resolved Quantum-Beat Spectroscopy with a Few-Cycle Pulse Laser. *IEEE J. Quantum Electron.* **2008**, *44*, 1232−1241.

(32) Kobayashi, T.; Nie, Z.; Du, J.; Okamura, K.; Kataura, H.; Sakakibara, Y.; Miyata, Y. Electronic Relaxation and Coherent Phonon Dynamics in Semiconducting Single-Walled Carbon Nanotubes with Several Chiralities. *Phys. Rev. B: Condens. Matter Mater. Phys.* **2013**, *88*, 035424.

DOI: 10.1021/acs.jpclett.5b01706
J. Phys. Chem. Lett. 2015, 6, 3560−3564